# Monte Carlo simulation of 2-dimensional $XY$ model

Qian Yuchen

May 12, 2025

**Abstract**

In this report, we will use Wolff cluster algorithm to investigate the basic behavior of 2-dimension $XY$ model. In particular, dynamic exponent $z$ of different sampling method, anomalous dimension $\eta(T)$, scaling behavior of correlation length $\xi(T)$ and thermodynamic properties will be carefully examined and compared with theory. The examination of Berezinskii-Kosterlitz-Thouless transition and vortex dynamics will also be involved.

## Contents



## List of Figures

# 1 Introduction

## 1.1 Physical background

It was well known by the physicists in the 1960s that two dimensional material lacks long range order, this later became the famous Mermin-Wagner theorem [4]. And it is expected that any two dimensional model with continues order parameter should not exhibit signs of phase transition. However, in the early 1970s, with further investigation of 2-dimensional $XY$ model using high-temperature series expansion, people realized the low temperature and high temperature behavior of such model are completely different.

To further illustrate such difference, let us consider the Hamiltonian of $XY$ model, its order parameter is given by planer vectors $\boldsymbol{S}$ with modular $|\boldsymbol{S}| = 1$:

$$\mathcal{H} = -\sum\nolimits_{\langle i,j\rangle} \boldsymbol{S}_i \cdot \boldsymbol{S}_j = -\sum\nolimits_{\langle i,j\rangle} \cos(\theta_i - \theta_j) \tag{1}$$

where $\theta_i \in [0, 2\pi)$ gives the direction of $\boldsymbol{S}_i$ in the $XY$ plane. The partition function is given by $\operatorname{Tr} \mathrm{e}^{-\mathcal{H}/T}$. Here for simplicity, coupling between nearest-neighbor spin is set to be 1 and $k_{\mathrm{B}} = 1$ as well. Then at 2-dimension, the correlation function of the spin $G(r) = \langle \boldsymbol{S_r} \cdot \boldsymbol{S_0} \rangle$ is given by

$$G(r) \sim \begin{cases} r^{-\eta(T)}, & \text{for } T \ll 1, \\ \mathrm{e}^{-r/\xi(T)}, & \text{for } T \gg 1. \end{cases} \tag{2}$$

When temperature is low, the correlation function has a power law decay. This is known as quasi-long-range-order (QLRO) given by the spin-wave approximation, as we shall discuss later. It differs from the usual symmetry breaking phase where the correlation exhibits a real long range order $G(r) \sim 1$ as $r \to \infty$. When the temperature is beyond the order of unity, such QLRO is again destroyed, leaving us with a exponential decay.

Later, Kosterlitz and Thouless [3] (and Berezinskii [1], independently) pointed out that when the temperature $T$ is above transition temperature $T_{\mathrm{KT}}$, the topological defect in $XY$ model, known as vortexes, starting to unbind,which causes QLRO to further break down. This is known as the Berezinskii-Kosterlitz-Thouless (BKT) transition. Kosterlitz and Thouless were rewarded the Nobel Prize in 2016 for this contribution.

## 1.2 Wolff Cluster Monte Carlo Algorithm

In this final project, we will use Monte Carlo method to examine the properties of BKT transition. From previous discussion, correlation function at low temperature is given by a power law decay. This is a sign that the system stays at the critical point, and renormalization group (RG) analysis shows the system stays on the fixed line of RG flow ar low temperature [7]. Hence normal Monte Carlo method like local update will experience critical slow down. So another method known as the Wolff cluster algorithm [8] will be adopted to speed up the program. The algorithm is as follows:

1. Choose a random angle $\phi$ and a random point $\boldsymbol{x}$ on the lattice as the first point of a cluster $C$ to be built.

2. Visit all nearest neighbor $\boldsymbol{y}$ of $\boldsymbol{x}$, add $\boldsymbol{y}$ to $C$ with probability

$$P = 1 - \mathrm{e}^{-\max\{0, \frac{2}{T}\cos(\phi - \theta_{\boldsymbol{x}})\cos(\phi - \theta_{\boldsymbol{y}})\}}. \tag{3}$$

   If $\boldsymbol{y}$ is added, visit all nearest-neighbor of $\boldsymbol{y}$ that is not in $C$. Try adding them to $C$. This recursively adds points to the cluster. Repeat this process until it stops.

3. Flip all the spin $\theta_{\boldsymbol{x}}$ with $\boldsymbol{x} \in C$ as $\theta_{\boldsymbol{x}} \to \pi - \theta_{\boldsymbol{x}} + 2\phi$.

The autocorrelation $C_{\mathrm{a}}(\tau) = \overline{\delta \boldsymbol{M}(t+\tau) \cdot \delta \boldsymbol{M}(t)}$ is estimated using the average magnetization at given time $\boldsymbol{M}(t) = L^{-2} \sum \boldsymbol{S}$, where $\delta \boldsymbol{M}(t) = \boldsymbol{M}(t) - \overline{\boldsymbol{M}}$ gives variance of average magnetization at time $t$. Let us compare the relaxation time of Wolff and local update by calculating the auto correlation $C_{\mathrm{a}}(\tau)$. The plot is given in figure(1). As one can see, Wolff is usually $10^2$ to $10^3$ times faster than local update.

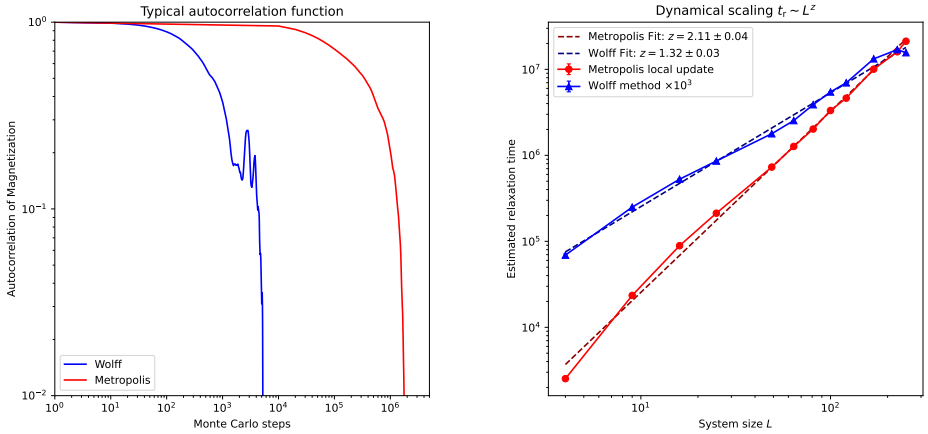


Figure 1: Left: A typical plot of $C_{\mathrm{a}}$ at $T = 1, L = 32$. Right: Scaling behavior of the relaxation time $t_{\mathrm{r}}$. Also note that data for Wolff update is scaled by $10^3$. The error is smaller than the size of the dot and take 100 sample is taken per point.

As suggested by [2], the relaxation time is given by $t_{\mathrm{r}} = \int_0^\infty \mathrm{d}\tau C_{\mathrm{a}}(\tau)/C_{\mathrm{a}}(0)$. In practice, the integral is cutoff when $C_{\mathrm{a}}(\tau)$ passes zero, which means $C_{\mathrm{a}}(\tau)$ has gone into fluctuation-dominated region. Also note that [8] when dealing with Wolff update, the average size of the cluster $\langle |C| \rangle$ should be considered in Monte Carlo step.

The actual determination of dynamical exponent for size $L$ system $t_{\mathrm{r}} \sim L^z$ turns out to be difficult. Here the monte carlo updates is done in temperature $T = 1$ and the fitting for the dynamical exponent $z$ is presented in figure(1). Each data point contains 30 sample. The fitted curve for metropolis method has $z = 2.11 \pm 0.04$, much larger than the Wolff exponent $z = 1.32 \pm 0.03$, proving the effectiveness of Wolff method.

## 1.3 Equilibrium test

The most tricky part of Monte Carlo simulation is to determine whether the result is in equilibrium. Suppose the physical quantity is given by $\mathscr{O}(t)$:

1. First, calculate the auto-correlation of $\mathscr{O}(t)$ as $C_{\mathscr{O}}(\tau)$. Pick the point where $|C_{\mathscr{O}}(\tau)|$ is smaller than the threshold 0.1, this is the estimated relaxation time $t_{\mathrm{r}}$. If such time does not exists, then this means $\mathscr{O}(t)$ is not in equilibrium.

2. Next, $\mathscr{O}(t)$ needs to estimated if they are truly independent as follows: first slice $\mathscr{O}(t)$ with $t_{\mathrm{r}}$. If such sample is too short, then nothing can be concluded from such data, so returns false. After slicing and using Kolmogorov-Smirnov test, datas are independent if $\mathsf{stat} < 0.1$ or $p > 0.01$. If such condition is satisfied, return True.

### 1.4 Optimize the program

The most time-consuming part is the cluster-building part. The program is speeded up by the following considerations:

- Change recursive deep first search to breadth first search (suggested by ai), so that we can use numba to speed up the program. This makes the program 5 times faster. Also we annotations all the data type so that numba is even faster by 1.2 times.
- Generate the random number outside the program. (Note that the largest possible cluster can only create $L^2$ attempts)
- When deciding adding the nearest neighbor of $\boldsymbol{x}$, we need to accept $\boldsymbol{y}$ with probability $1-\mathrm{e}^{-\max\{0,\frac{2}{T}\cos(\phi-\theta_{\boldsymbol{x}})\cos(\phi-\theta_{\boldsymbol{y}})\}}$. This is to say, we accept $\boldsymbol{y}$ if

  $$1-\mathrm{e}^{-\max\{0,\frac{2}{T}\cos(\phi-\theta_{\boldsymbol{x}})\cos(\phi-\theta_{\boldsymbol{y}})\}}>r, \tag{4}$$

  for random number $r$ in $[0,1]$. This can be further simplified with following consideration: the above inequality is equivalent to $1-r>\min\{1,\mathrm{e}^{-\frac{2}{T}\cos(\phi-\theta_{\boldsymbol{x}})\cos(\phi-\theta_{\boldsymbol{y}})}\}$. Now $1-r=r'$ is still an random number in $[0,1]$. The above inequality is equivalent to $r'<\mathrm{e}^{-\frac{2}{T}\cos(\phi-\theta_{\boldsymbol{x}})\cos(\phi-\theta_{\boldsymbol{y}})}$ for $r'\in[0,1]$, so we do not need to take min in the actual program, hence the above inequality further simplifies to

  $$-\frac{T}{2}\ln(r')<\cos(\phi-\theta_{\boldsymbol{x}})\cos(\phi-\theta_{\boldsymbol{y}}), \tag{5}$$

  evaluation of left hand side can be done in array style and hence is faster by 1.1 times. Another trick is to record $\cos(\phi-\theta_{\boldsymbol{x}})$ outside the for loop for nearest neighbor.

Another time-consuming part is to check if the data is in equilibrium, since it needs to calculate auto-correlation:

- Usually more than 1000 data point is collected before it is accepted as in equilibrium. So the program directly return false if the data point is less than 500.
- Instead of checking it every time, check equilibrium after recording 10 new data.
- Quit the loop after 10000 evaluation to prevent it stuck inside the loop.

# 2 Low Temperature Phase: Spin Wave Approximation and Beyond

In this section, we shall discuss the low-temperature behavior of $XY$ model. When $T\ll 1$, $\theta$ varies slowly in space, and hence the difference of $\theta$ at nearest neighbor is small. We may approximate the Hamiltonian as $\frac{1}{2}\sum_{\langle i,j\rangle}(\theta_i-\theta_j)^2+\text{const}$, which is referred as spin wave approximation, in the sense that only spin wave excitation is considered. Now symmetry is manually broken by assuming $\theta$ fluctuates around $\theta=0$, then the action is Gaussian. Taking Fourier transformation, the Hamiltonian is given by $\sum_{\boldsymbol{k}}\theta_{-\boldsymbol{k}}(4-2\cos k_x-2\cos k_y)\theta_{\boldsymbol{k}}$ and hence $\theta$-correlation is given as

$$\tilde{C}(\boldsymbol{r})=L^{-2}\sum\nolimits_{\boldsymbol{k}}\frac{\mathrm{e}^{\mathrm{i}\boldsymbol{k}\cdot\boldsymbol{r}}-1}{4-2\cos k_x-2\cos k_y}. \tag{6}$$

where $\boldsymbol{k}$ sums over the first Brillouin zone and it is normalized as $\tilde{C}(0)=0$. One can obtain useful information from this $\theta$-correlation [5], as we shall discuss in detail below.

## 2.1 Thermodynamic properties

Let us first discuss the thermodynamic properties of $XY$ model using such approximation. In particular, one may directly obtain [5] quantities like average magnetization $M = L^{-2}|\sum_i \boldsymbol{S}_i|$, average energy per site $E$, susceptibility $\chi = T^{-1}\langle M^2\rangle$ and specific heat $C_V$:

$$\langle M\rangle = 1 - \eta(\ln 2L_{\text{eff}}^2)/4, \qquad \chi = L_{\text{eff}}^{-\eta}, \tag{7}$$

$$E = 2 - T/2, \qquad C_V = 1/2 \tag{8}$$

where $\eta = T/2\pi$ is the anomalous dimension predicted by spin wave approximation and $L_{\text{eff}}$ is the effective system size. These prediction matches the numerical result, except that the effective system size $L_{\text{eff}}$ in the formula is 2.2 times larger than the size of real system. The plot of these quantities are given in figure(2)

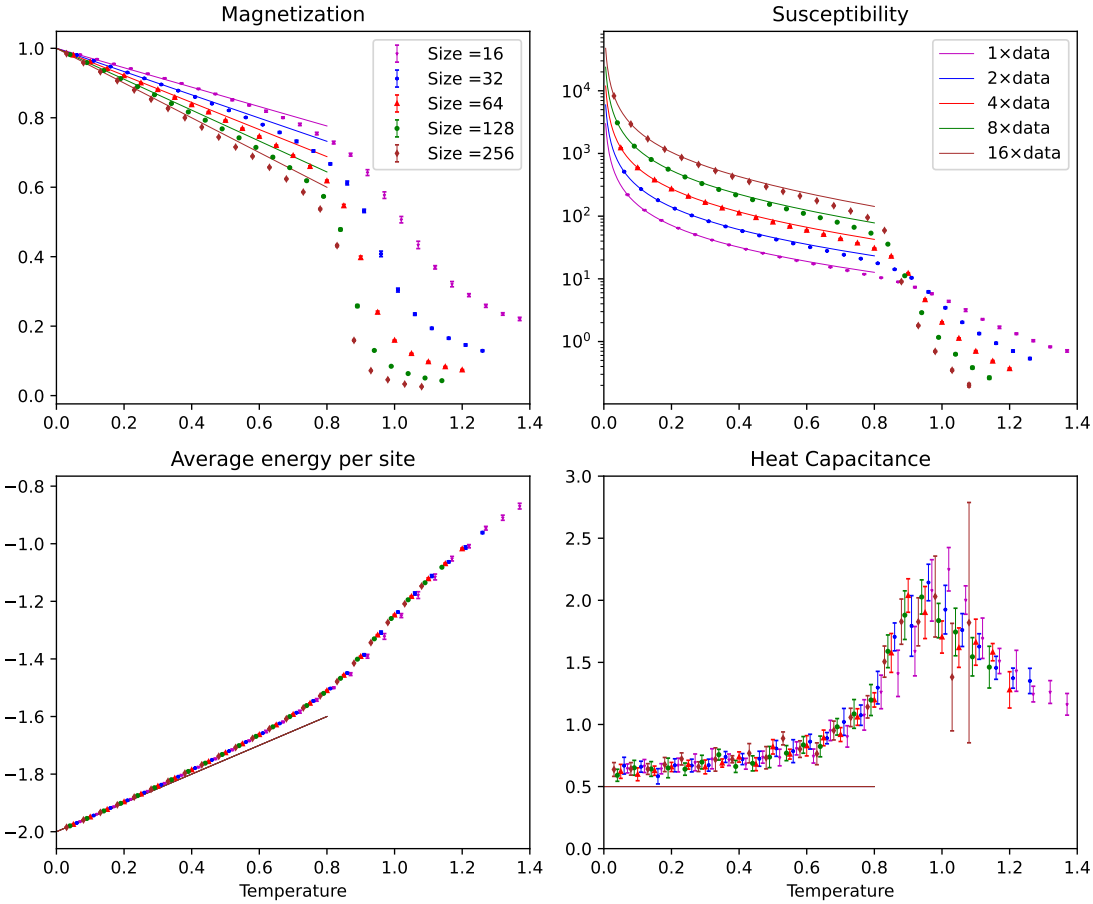


Figure 2: Monte Carlo simulation of thermodynamic properties. Solid line comes from the prediction from equation (7) to (8) with replacement $L_{\text{eff}} = 2.2L$. Data in susceptibility plot are shifted. 10 Samples are taken per datapoint.

$E$ and $C_V$ almost do not depend on the size of the system, and $C_V$ is still continues near the transition temperature $T_{\text{KT}}$. The peak around $T = 1.1$ differs from the actual critical point and is not related to the phase transition. This is the main difference BKT transition from normal phase transition.

Also, $\chi = T^{-1}\langle M^2\rangle \sim L^{-\eta}$ exhibits power law relaxation with system size $L$. After taking thermodynamical limit $L \to \infty$ at $T > 0$, $\chi \to 0$ and there is no magnetization, thus is consistent with Mermin-Wagner theorem. As one may recall, the QLRO is given by

the condensation of spin waves: the spin wave density is given by $\int_{1/L}^{1/a} \mathrm{d}^2k/k^2 \sim \ln(L/a)$ where $a$ is the size of the lattice. For finite system, spin wave density does not diverge since the momentums near $\boldsymbol{k} = 0$ are bounded, phase transition only happens when $L \to \infty$. Also note that this $\ln L$ divergence is still rather weak, as one may observe in the plotting: double the system size $L$ will only cause linear change on the slope of $\langle M \rangle$ and $\ln \chi$.

## 2.2 Anomalous Dimension and Correlation

Next, let us discuss the scaling behavior of correlation function. It is well known that the spin correlation is given as $r^{-\eta}$. At low temperature, the correlation function experience power law decay, as predicted by the spin wave approximation. In figure(3) we present plots for correlation $G(r)$.

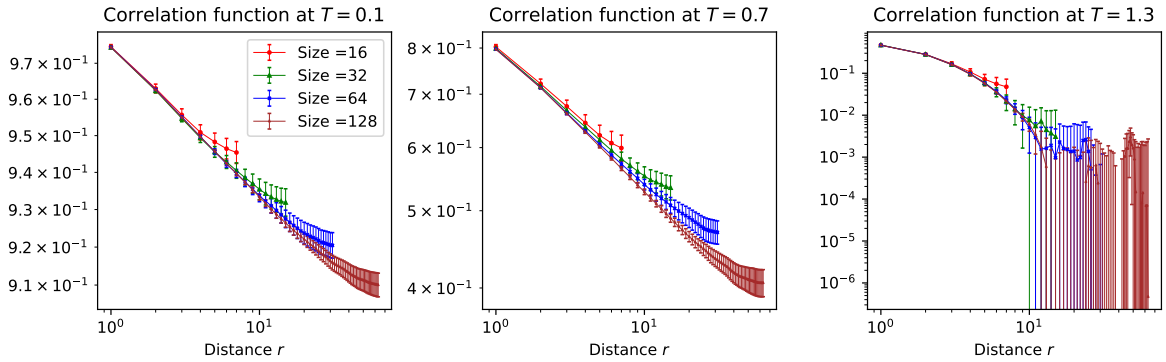


Figure 3: Log-Log plot of correlation function $G(r)$ at three different temperature. Note that $r$ ranges from 1 to $L/2$. $T = 0.1$ and $T = 0.7$ are below $T_{\mathrm{KT}}$ while $T = 1.3$ is above $T_{\mathrm{KT}}$, hence $G(r)$ no longer scales as $r^{\eta(T)}$. For each point we take 50 samples.

When $T < T_{\mathrm{KT}}$, spin correlation exhibits universal scaling behavior, as one can clearly see from the identical $G(r)$-$T$ plot at $T = 0.1$ and $T = 0.7$, which also includes the finite size effect. As pointed out by [5], the correlation function is given by $G(r) = \mathrm{e}^{2\pi\eta(T)\tilde{C}(r)}$ where $\tilde{C}(r)$ in equation(6) is the universal (independent of $T$) lattice $\theta$-correlation. We will use this method to estimate $\eta(T)$ value. Note that both $\tilde{C}(r)$ and $G(r)$ takes $L^2$ different value for each configuration, this actually gives $L^2$ different estimation of $\eta(T)$.

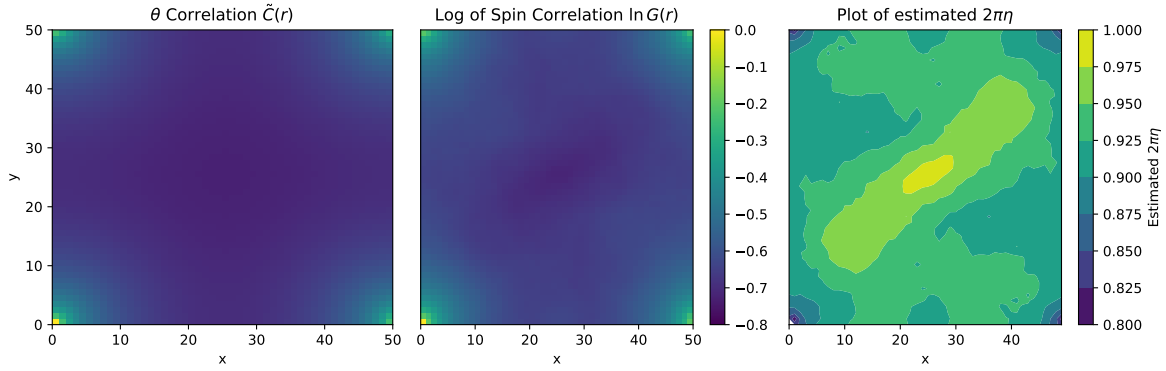


Figure 4: Plot of $\tilde{C}(\boldsymbol{r})$, $\ln G(\boldsymbol{r})$ and $\ln G(\boldsymbol{r})/C(\boldsymbol{r})$. Last one gives an estimation of $2\pi\eta$. We take $T = 0.65, L = 50$ and average $G(r)$ over 20 configurations. The error at the corner is caused by $C(\boldsymbol{r}) \to 0$.

See figure(4) for plot of $\tilde{C}(\boldsymbol{r})$, $\ln G(\boldsymbol{r})$ and estimated $\eta(\boldsymbol{r})$.

Another method to estimate $\eta(T)$ is to use the relation $\langle M^2 \rangle \sim L^{-\eta}$, as suggested by [2]. First we evaluate $\langle M^2 \rangle$ at same temperature but different size, then use linear regression to fit the curve. Here we give a plot in figure(5) using both method. It is

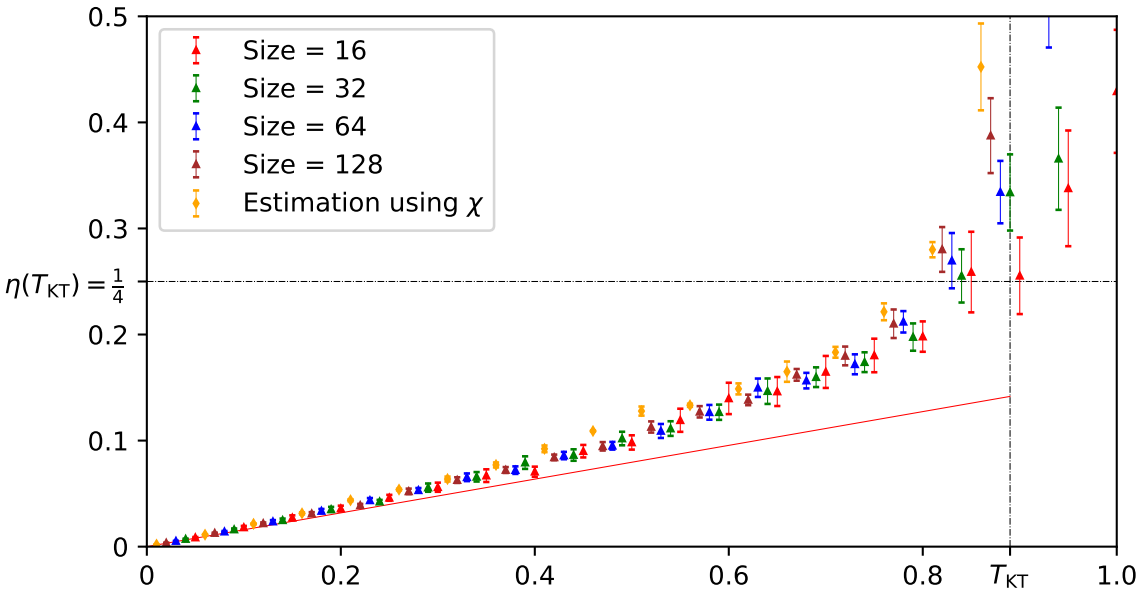


Figure 5: Estimated $\eta(T)$. For estimation using $\tilde{C}(r)$, we took 30 samples per point. For estimation using $\chi$, we take $L = 16, 32, 48, 64, 80, 100$ to make the fitting. The red solid line is given as the spin wave contribution $\eta(T) = T/2\pi$.

interesting to note that these two method do not agree at high temperature regime. This is possibly because the correlation $\tilde{C}(r)$ is derived within spin wave approximation and the relation between $\tilde{C}(r)$ and $G(r)$ is no longer valid. However, the relation $\chi \sim L^{-\eta}$ comes from finite size scaling and does not depend on spin wave approximation.

When $T > 0.6$, $\eta(T)$ already deviates from the spin wave approximation. The transition temperature $T_{\mathrm{KT}} = 0.89$ from [8], and the universal exponent $\eta(T_{\mathrm{KT}}) = \frac{1}{4}$ from [3] are also labeled. It is predicted that at the critical point $T_{\mathrm{KT}}$, $\eta$ should equal $\frac{1}{4}$ in figure(5). This agrees with the numerics within some errors.

# 3 High Temperature Phase: the Transition and Vortex Dynamics

In the previous section, we studied the basic properties of $XY$ model in low temperature using spin wave approximation. We have seen that as the temperature is beyond the order of unity, there are signs of phase transitions, including but not limit to: a sudden drop in $\langle M \rangle$ and $\chi$, different scaling behavior of correlation and increasing error when evaluating $\eta$. All these signs indicates the spin wave approximation no longer applies, and the QLRO is destroyed. In this section, we will discuss the basic properties of such transition.

The nature of such transition comes from the unbind of vortex pairs. In singe-particle level, the free energy of one vortex is given as $(\pi - 2T)\ln(L/a)$, and hence the transition temperature is roughly at $T_{\mathrm{KT}} = \pi/2$. Above such temperature, the vortex began to unbind. In this section we will determine the basic properties of such transition.

## 3.1 Determine Critical Temperature

Let us determine the critical temperature $T_{\mathrm{KT}}$. As pointed out by [6], the determine of $T_{\mathrm{KT}}$ uses helicity modulus, defined as

$$\Upsilon_L(T) = -\frac{1}{2L^2}\langle \mathcal{H} \rangle - \frac{1}{TL^2}\left\langle \left( \sum\nolimits_{\langle ij \rangle} \sin(\theta_i - \theta_j)\hat{\boldsymbol{e}}_{ij} \cdot \hat{\boldsymbol{x}} \right)^2 \right\rangle, \tag{9}$$

where $\hat{\boldsymbol{e}}_{ij}$ points from $i$ to $j$. Let $L \to \infty$, $T_{\mathrm{KT}}$ is given by the intersection of $\Upsilon_\infty(T)$ and $2T/\pi$.

Another popular way to determine the critical temperature is to use the binder ratio

$$B_L = 1 - \langle M^4 \rangle_L / 3 \langle L^2 \rangle_L \tag{10}$$

where $\langle \ldots \rangle_L$ sums over size-$L$ system. For different $L$, $B_L(T)$ will coincide at $T_{\mathrm{c}}$, giving us the critical temperature.

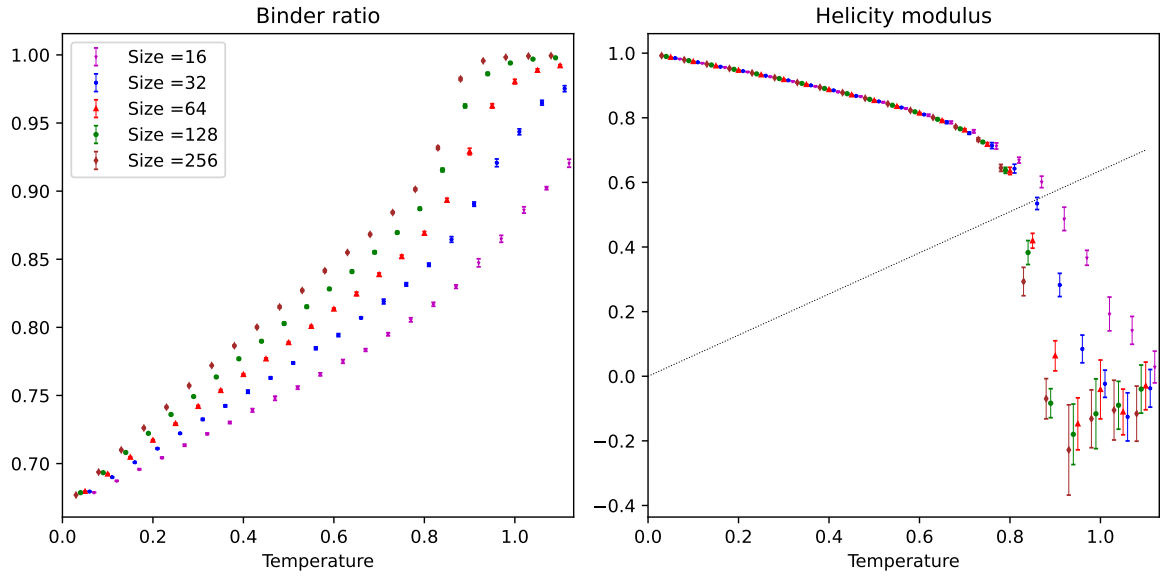


Figure 6: $B_L$ and $\Upsilon_L$. We take 15 samples per point. The line $2T/\pi$ are also drawn.

The plot of $B_L$ and $\Upsilon_L$ are given in figure(6). It is notable that $B_L$ cannot capture the transition temperature $T_{\mathrm{KT}}$, and it predicts the transition happens at $T = 0$, which is indeed the case. When the system turns into finite temperature, spin wave emerges, breaking the magnetic order, which is similar to the famously known $1d$ Ising case. This gives another reason why BKT transition is different from ordinary order-disorder phase transition within the Landau theory and falls into another category of phase transition, known as topological phase transition.

From the $\Upsilon_L$ plot, as $L \to \infty$, different $\Upsilon_L$ differs as temperature rises. For $L = 256$, the estimated transition temperature should be round $T_{\mathrm{KT}} \simeq 0.8$.

Also, as mentioned before, $\eta = \frac{1}{4}$ already gives an result for $T_{\mathrm{KT}}$ since it is the universal exponent at critical temperature [2, 3]. As one can read from figure(5), $\eta(T)$ crosses $\frac{1}{4}$ around $T = 0.8$.

One may also use the scaling relation $\Upsilon_L/\Upsilon_\infty = 1 + 1/(C + \ln L)$to fit $\Upsilon_\infty$ by adjusting $C$ to minimize the square of error. The result is given in figure(7), we get $T_{\mathrm{KT}} = 0.80 \pm 0.01$.

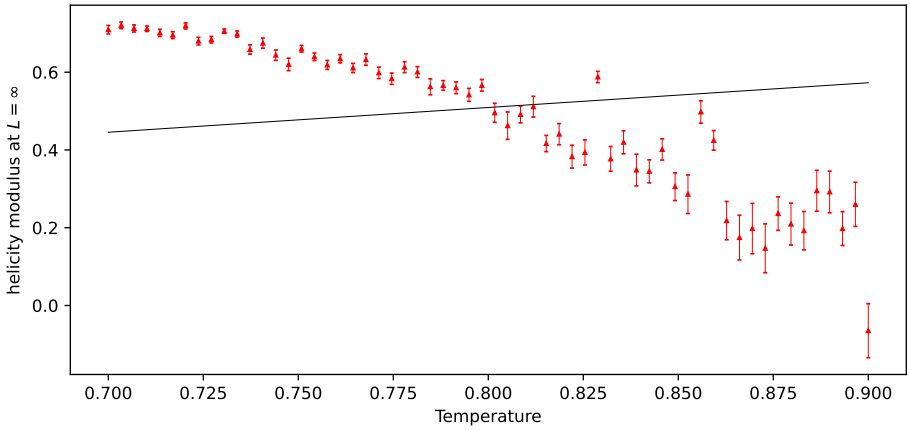


Figure 7: Fitted $\Upsilon_\infty$ using finite size results. We used $L = 4, 8, 12, \ldots, 100$ to fit the result, and for each finite size result, 20 data points are taken.

These three methods agrees pretty well, except that the $T_{\mathrm{KT}}$ we estimate is round 0.8, instead of 0.9, as recorded in most references, and I am not sure about why such deviation is observed.

## 3.2 Correlation Length and Scaling Behavior

As mentioned before, when $T > T_{\mathrm{KT}}$, the correlation is given as exponential decay $\mathrm{e}^{-r/\xi}$, where $\xi$ gives the correlation length. We give a plot of $G(r)$ above $T_{\mathrm{KT}}$ at figure(8). If we

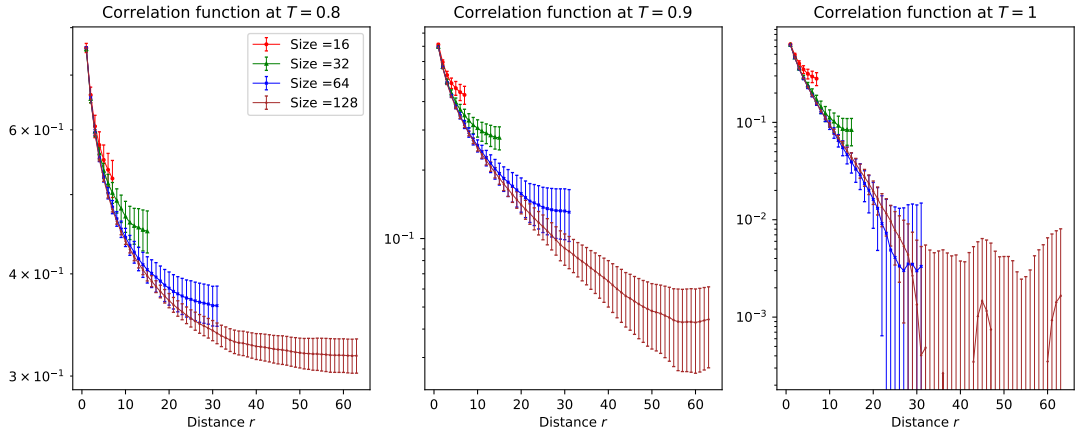


Figure 8: Plot of $G(r)$ at high temperature. Clearly one can see the finite-size effect as $T \to T_{\mathrm{KT}}$ since $\xi \gg L$.

measure $G(r)$ along the $x$ axis, then $G(r)$ has $L$-periodicity, and we may include finite-size effect by taking the ansatz that $G(r) = \mathrm{e}^{\eta \tilde{C}(r)}(\mathrm{e}^{-r/\xi} + \mathrm{e}^{(r-L)/\xi})$, suggested by [5]. Actually, we will use a more complicated form

$$G(\boldsymbol{r}) = \mathrm{e}^{\eta \tilde{C}(\boldsymbol{r})} \left( \mathrm{e}^{-\sqrt{x^2+y^2}/\xi} + \mathrm{e}^{-\sqrt{(L-x)^2+y^2}/\xi} + \mathrm{e}^{-\sqrt{x^2+(L-y)^2}/\xi} + \mathrm{e}^{-\sqrt{(L-x)^2+(L-y)^2}/\xi} \right), \tag{11}$$

to do the fitting. $\xi$ and $\eta$ are determined by minimizing the square of error between such form and measured data.

In theory this should works well. However, in practice, the fitting is not very good. In fact, minimizing the square of error is not a good idea using gradient decent method. I also plotted the $error(\xi, \eta)$ plot, and the result is not very satisfying since the details tend to be vague, and I do not attatch the plot in this report. (However you can find it in the code.)

## 3.3 Detection of Vortex

In this section, let us discuss how do we detect vortex in an lattice system. In continuum description, the charge $q$ of the vortex is given as $\oint \nabla\theta \cdot \mathrm{d}\boldsymbol{r} = 2\pi q$, where the center of vortex falls in the contour. In the discrete lattice description, the integration is replaced by a summation over edges of plaquette: $\sum_{\square}(\Delta\theta)_{ij}$, where $(\Delta\theta)_{ij}$ defined on bonds is the difference of $\theta$ between nearest neighbor $i$ and $j$. If we directly take that as the definition, the summation over plaquette will cancel out and the charge is always zero. Hence, instead, we replace $\Delta\theta$ by $\widetilde{\Delta\theta} \in [-\pi, \pi]$ in the summation, which is adding a integer multiplier of $2\pi$ to $\Delta\theta$ so that it falls in $[-\pi, \pi]$. The idea behind such definition is that $\theta$ is actually defined modular $2\pi$, and hence $\widetilde{\Delta\theta}$ are chosen within the principle branch $[-\pi, \pi]$.

Hence, the summation $\sum_{\square} \widetilde{\Delta\theta}$ will be an integer multiplier of $2\pi$, and $\widetilde{\Delta\theta} \in [-\pi, \pi]$ implies the summation can only be $\pm 2\pi$ and 0, corresponding to the charge of $\pm 1$, a vortex and 0, the trivial spin waves. (The case of $\pm 4\pi$ is very unlikely to happen.) This give us the desired topological charge of vortex. Indeed numerical calculation shows such summation can only be $\pm 2\pi$ or 0, within the rounding error of $\sim 10^{-16}$. Here we present a series of spin and vortex at different temperature in figure(9)

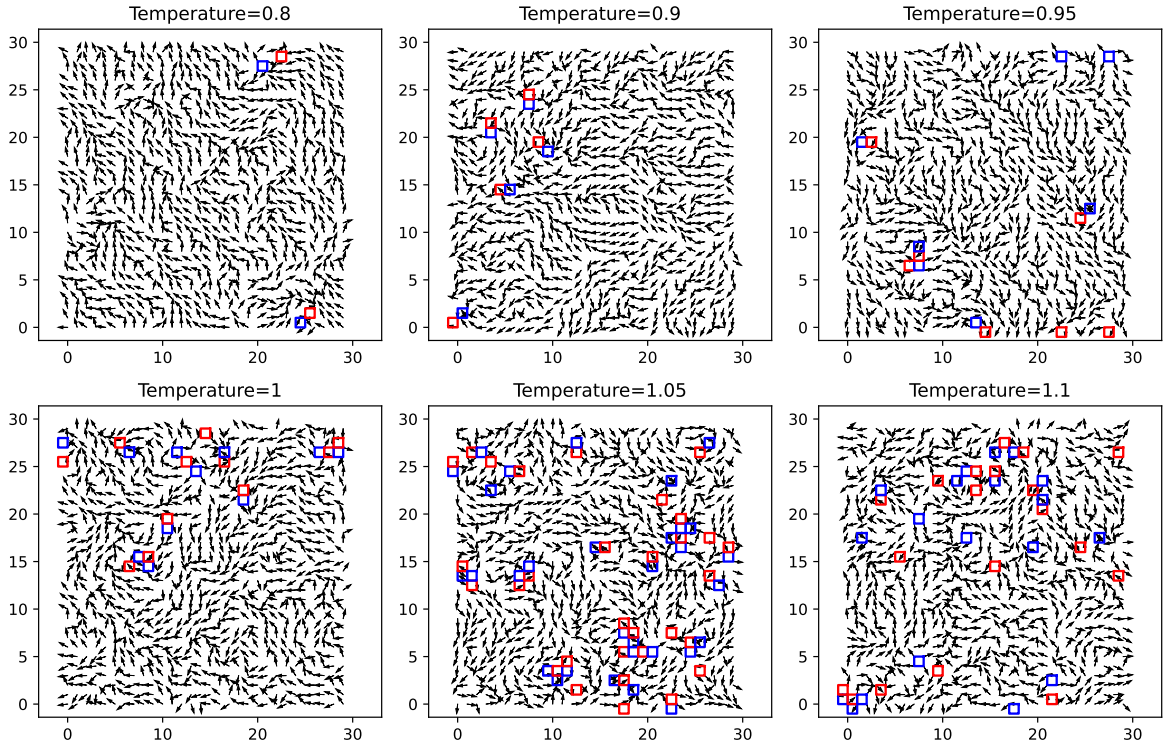


Figure 9: Typical $XY$ spin configuration and the distribution of vortexes at different temperature. Red squares are for vortexes while blue squares are for anti-vortexes.

When the temperature is below $T_{\mathrm{KT}}$, vortexes are grouped together, and its number are

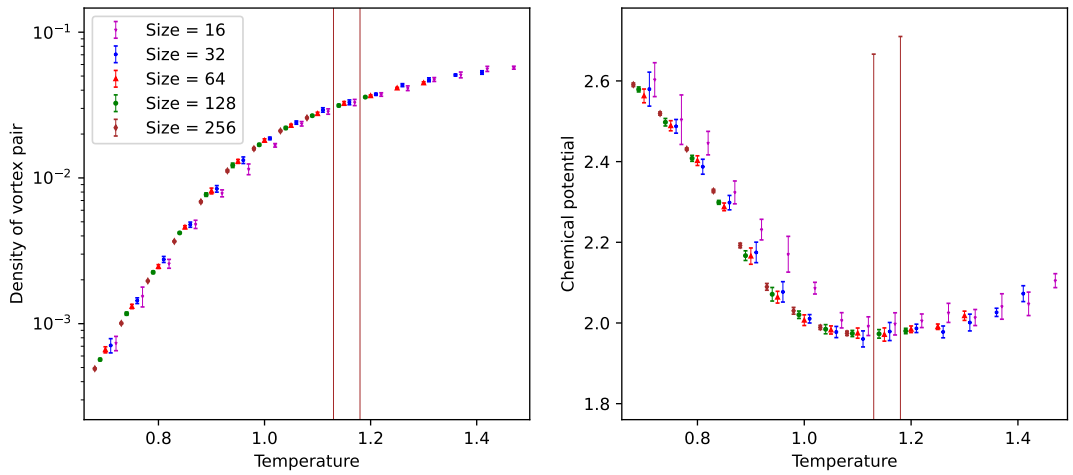


Figure 10: Vortex pair density $n_v$ and chemical potential $\mu$. We take 10 sample per point. Except $L = 16$ case, the result do not have significant scale dependence.

suppressed. As the temperature increases, such excitation emerges, and pairs of vortexes begin to unbind, as predicted by the BKT theory.

It is also notable that, the initial configuration is set to be a uniform magnetization field $\boldsymbol{S} = \text{const}$, and hence the initial topological charge of the field is zero. As we update the spins, the vortex and anti-vortex should appear together by their topological nature. And hence the number of vortex and anti-vortex should always equal, as one may seen from the above figure(9).

As suggested by [5], the density of vortex paris, within single particle approximation, is given by $n_v = \mathrm{e}^{-2\mu/T}$, where $\mu$ is the chemical potential (or gap) of single vortex. Here we present a plot of $n_v$ and $\mu$ in figure(10).

As one may notice, the vortex density grows exponentially as $T \to T_{\mathrm{KT}}$ from the low temperature phase, and the chemical potential $\mu$ drops linearly. This is consistent with the picture we saw, meaning that indeed, the vortex began to unbind easily when $T > T_{\mathrm{KT}}$. However, when $T > T_{\mathrm{KT}}$, the vortex density tends to a constant while the chemical potential seems unchanged. This is because the vortex also experience an interaction energy of $q_1 q_2 \ln r_{12}$, where $q$ are the charge of the vortex, and $r_{12}$ is the distance between them. This increasing energy from existing vortexes suppressed the vortex paris from emerging, and the single particle approximation no longer applies.

# 4 Conclusion

In this report, we have used Wolff cluster algorithm to investigate the basic properties of 2-dimensional $XY$ model. We have seen that the spin wave approximation works well at low temperature, and the anomalous dimension $\eta(T)$ is given by $T/2\pi$. The correlation function exhibits power law decay, and the average magnetization and susceptibility are also calculated.

We also discussed the BKT transition and the nature of such transition. The critical temperature $T_{\mathrm{KT}}$ is determined using helicity modulus, binder ratio and scaling relation.

However, in the numerical simulation, we found that the transition temperature $T_{\mathrm{KT}}$ is lower than the theoretical value, inconsistent with the result from [8] and most references.

Also we tried to fit the correlation function at high temperature using the ansatz

$G(r) = \mathrm{e}^{\eta \tilde{C}(r)}(\mathrm{e}^{-r/\xi} + \mathrm{e}^{(r-L)/\xi})$, but the fitting is not very good. This is possibly because the finite size effect is not well captured by such ansatz, or there is some wrong with the fitting method.

Finally, we also discussed the vortex dynamics and its density. The density of vortex pairs is given by $n_v = \mathrm{e}^{-2\mu/T}$, where $\mu$ is the chemical potential of single vortex. The density of vortex pairs grows exponentially as $T \to T_{\mathrm{KT}}$ from low temperature phase, and the chemical potential drops linearly.

# References


[1] V. L. Berezinskiĭ. Destruction of Long-range Order in One-dimensional and Two-dimensional Systems Possessing a Continuous Symmetry Group. II. Quantum Systems. Soviet Journal of Experimental and Theoretical Physics, 34:610, January 1972.

[2] Julio F. Fernández, Manuel F. Ferreira, and Jolanta Stankiewicz. Critical behavior of the two-dimensional xy model: A monte carlo simulation. Phys. Rev. B, 34:292–300, Jul 1986.

[3] J. M. Kosterlitz and D. J. Thouless. Ordering, metastability and phase transitions in two-dimensional systems. Journal of Physics C Solid State Physics, 6(7):1181–1203, April 1973.

[4] N. D. Mermin and H. Wagner. Absence of ferromagnetism or antiferromagnetism in one- or two-dimensional isotropic heisenberg models. Phys. Rev. Lett., 17:1133–1136, Nov 1966.

[5] Jan Tobochnik and G. V. Chester. Monte carlo study of the planar spin model. Phys. Rev. B, 20:3761–3769, Nov 1979.

[6] Hans Weber and Petter Minnhagen. Monte carlo determination of the critical temperature for the two-dimensional xy model. Phys. Rev. B, 37:5986–5989, Apr 1988.

[7] Xiao-Gang Wen. Quantum Field Theory of Many-Body Systems: From the Origin of Sound to an Origin of Light and Electrons. Oxford University Press, 09 2007.

[8] Ulli Wolff. Collective monte carlo updating for spin systems. Phys. Rev. Lett., 62:361–364, Jan 1989.